Asian J Biol Life Sci., 2026; 15(2):559-566.
https://ajbls.com

Research Article

Experimental and Computational Data on Indazole-Pyridine Derivatives: Synthesis, Characterization, and Anticancer Evaluation

Kinjal Parmar[1,*], Ishan Panchal[2]

[1]Faculty of Pharmacy, Parul University, Limda, Waghodia, Vadodara, Gujarat, INDIA.
[2]Department of Pharmaceutical Chemistry, Parul College of Pharmacy and Research, Faculty of Pharmacy, Parul University, Bopal, Ahmedabad, Gujarat, INDIA.

ABSTRACT

Introduction: Breast cancer remains a major cause of cancer-related mortality among women worldwide, highlighting the need for novel therapeutic agents. **Materials and Methods:** Two indazole-pyridine derivatives (7i and 7j) were synthesized and characterized using FTIR, ^{1}H-NMR, ^{13}C-NMR, and mass spectrometry. Molecular docking was performed to evaluate binding interactions. *In vitro* cytotoxicity against the MCF-7 cell line was assessed using the SRB assay (10-80 µg/mL). **Results:** Docking studies indicated stable ligand-receptor interactions. Both compounds exhibited dose-dependent cytotoxicity. Compound 7j showed strong antiproliferative activity (GI_{50}<10 µg/mL), while compound 7i showed moderate activity (GI_{50}=33.6 µg/mL). **Conclusion:** The presence of a pyrrolidine moiety in 7j enhances activity. These derivatives represent promising scaffolds for further optimization as anticancer agents.

Keywords: Indazole-Pyridine Derivatives, MCF-7 cell line, Molecular Docking, Structure-activity Relationship.

Correspondence:
Ms. Kinjal Parmar
Research Scholar, Faculty of Pharmacy, Parul University, Limda, Waghodia, Vadodara-391760, Gujarat, INDIA.
Email: kinjal.parmar19149@paruluniversity.ac.in

Received: 14-05-2026;
Revised: 08-06-2026;
Accepted: 24-07-2026.

INTRODUCTION

Cancer is a major global health concern characterized by uncontrolled cell growth and proliferation, leading to severe physiological complications. Despite advancements in diagnosis and treatment, it remains a leading cause of mortality worldwide (Siegel *et al*., 2024). Among various cancers, breast cancer is one of the most commonly diagnosed malignancies in women and continues to pose a significant burden, especially in developing countries like India (Giaquinto *et al*., 2024; Kulothungan *et al*., 2024). Targeted therapies have improved treatment outcomes; however, challenges such as drug resistance and toxicity highlight the need for novel therapeutic agents (Knight *et al*., 2021; Roy and Li, 2016; Abbas and Rehman, 2018; Charmsaz *et al*., 2019; Arruebo *et al*., 2011). Tropomyosin receptor kinase A (TrkA) has emerged as an important target in breast cancer, as its activation is associated with tumor progression, survival, and metastasis. Neurotrophins such as Nerve Growth Factor (NGF) play a key role in activating TrkA signaling pathways (Descamps *et al*., 2001; Com *et al*., 2007; Noh *et al*., 2013; Helal *et al*., 2015; Martin-Zanca *et al*., 1986; Descamps *et al*., 2001). Indazole and pyridine scaffolds are widely recognized for their pharmacological potential, particularly in anticancer drug development. Several FDA-approved drugs containing these moieties have demonstrated significant therapeutic efficacy, making them promising candidates for further exploration (Davidson *et al*., 2004; Youssef *et al*., 2014; DiGiulio, 2013; Cui *et al*., 2011). The clinical success of TRK inhibitors has significantly advanced targeted cancer therapy. Entrectinib has demonstrated efficacy against NTRK, ROS1, and ALK fusion-positive tumors, including non-small-cell lung cancer (Liu *et al*., 2018; Drilon *et al*., 2020), while larotrectinib has shown high selectivity and effectiveness in TRK fusion-driven malignancies (André *et al*., 2019; Federman and McDermott, 2019). Furthermore, NTRK genes have been identified as key oncogenic drivers in various solid tumors, including breast cancer (Lu *et al*., 2022; Berlin *et al*., 2020). The FDA approval of these agents has stimulated growing interest in the development of novel TRK-targeted therapeutics (Skerratt *et al*., 2016). In this context, the design of new indazole-pyridine derivatives represents a promising strategy for developing effective anticancer agents targeting TRK-associated pathways. In the present study, two novel indazole-pyridine derivatives (7i and 7j) were designed, synthesized, and evaluated for their anticancer potential against the MCF-7 breast cancer cell line. Molecular docking studies were also performed to investigate

OPEN ACCESS

Manuscript TECHNOMEDIA

DOI: 10.5530/ajbls.20260139

their interaction with the TrkA target protein. The aim of this study is to design and synthesize indazole-pyridine derivatives (7i and 7j) and evaluate their anticancer activity using *in vitro* and molecular docking approaches targeting the TrkA receptor.

MATERIALS AND METHODS

Materials

All chemicals and reagents were procured from commercial sources, including Sigma-Aldrich, Loba Chemie, and Spectrochem, and were used without further purification. Reaction progress was monitored by Thin-Layer Chromatography (TLC) on silica gel 60 F254 precoated aluminum plates and visualized under UV light or iodine vapor. Melting points were determined in sealed capillaries using a Gallenkamp apparatus and are uncorrected. Infrared (IR) spectra were recorded using a Bruker Optics Alpha II FTIR spectrometer by the KBr pellet method. 1H and 13C NMR spectra were obtained on a Bruker Avance II 400 MHz spectrometer using $CDCl_3$ or DMSO-d_6 as solvents, with chemical shifts (δ) expressed in ppm and coupling constants (J) in Hz. Mass spectral analysis was performed using electrospray ionization (ESI-MS) on a Bruker MicroTOF spectrometer. All reactions were carried out using anhydrous solvents under standard laboratory conditions. *In vitro* biological studies were conducted at the Tata Institute of Fundamental Research (TIFR), Mumbai, India.

Reagents and Conditions: (a) ethanol at rt for 10 min; (b) hydrazine hydrate (NH_2NH_2·H2O), reflux for 12 hr; (c) dry DMF, HOBt and EDC·HCl at rt, stirring, 8 hr; (d) dry dioxane at rt stir for 15 min; (e) DPPE, NaOtBu, and $Pd(OAc)_2$ at 50°C stirring for 30 min; (f) pyrrolidine (7j), and morpholine (7i) in an oil bath at 90°C for 8-20 hr.

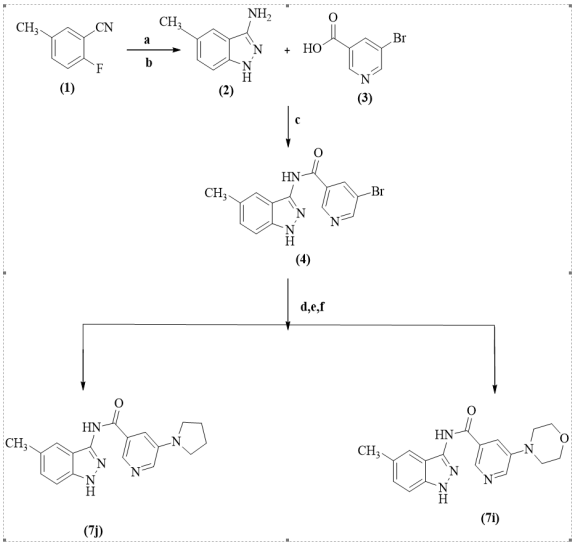

Scheme: Synthesis of Indazole based derivatives.

Methods

5-Methyl-1H-indazol-3-amine (2)

Compound 1 (0.1 mol) was dissolved in ethanol (20 mL) in a 25 mL round-bottom flask and stirred at room temperature for 10 min. Hydrazine hydrate (2 equiv.) was then added, and the reaction mixture was refluxed in an oil bath for 12 hr. The progress of the reaction was monitored by Thin-Layer Chromatography (TLC) using ethyl acetate:hexane (3:7) as the mobile phase. Upon completion, the solvent was removed under reduced pressure, and the resulting product was collected, dried, and purified by recrystallization to obtain 5-methyl-1H-indazol-3-amine (2) as a white crystalline solid. Yield: 76%; m.p.: 192-194°C (lit. 193-195°C); R_f: 0.60 (ethyl acetate:hexane, 3:7). IR (KBr, ν cm^{-1}): 3398, 3325 (N-H), 3020 (Ar-C-H), 2913 (aliphatic C-H), 1621 (C=N), 1504 (C=C). ESI-MS (m/z): 147.5 $[M]^+$.

Synthesis of (3-amino-5-methyl-1H-indazol-1-yl) (5-bromopyridin-3-yl)methanone (4)

5-Bromopyridine-3-carboxylic acid (3) (0.1 mol) was dissolved in dry DMF (10 mL) in a 25 mL round-bottom flask. To this solution, HOBt (0.2 mol) and EDC·HCl (0.2 mol) were added, and the mixture was stirred at room temperature for 30 min. Subsequently, 5-methyl-1H-indazol-3-amine (2) (0.1 mol) was added, and the reaction mixture was stirred for 8 hr at room temperature. After completion, the reaction mixture was poured into cold water, and the resulting precipitate was filtered, dried, and purified by recrystallization from 95% ethanol to afford compound (4) as white crystalline solid. Yield: 65%; m.p.: 220-224°C. IR (KBr, ν cm^{-1}): 3434, 3312 (N-H), 3065 (Ar-C-H), 1669 (C=O), 1580 (C=N), 1556 (C=C), 691 (C-Br). ^{1}H-NMR ($CDCl_3$, δ ppm): 2.45 (s, 3H, CH_3), 7.44-7.47 (m, 4H, Ar-H), 8.23-8.51 (d, 1H, Ar-H), 8.51 (s, 1H, Ar-H). ESI-MS (m/z): 332.18 $[M]^+$.

Synthesis of (7i-7j)

Intermediate (4) (0.1 mol) was dissolved in dry dioxane (3 mL) in a round-bottom flask and stirred at room temperature for 15 min. To this, 1,2-bis(Diphenylphosphino)Ethane (DPPE, 0.01 mol), sodium tert-butoxide (NaOtBu, 1 mol), and palladium acetate ($Pd(OAc)_2$, 0.1 mol) were added. The reaction mixture was stirred at 50°C for 30 min under inert conditions.

Subsequently, the appropriate amine (0.12 mol) was added, and the reaction mixture was heated at 90°C for 8-20 hr. After completion, the mixture was poured into ice-cold water, and the precipitated product was filtered, dried, and recrystallized from 95% ethanol to obtain the final compounds (7i and 7j).

(3-amino-5-methyl-1H-indazol-1-yl) (5-morpholinopyridin-3-yl)methanone (7i)

White crystalline solid; Yield: 67%; m.p.: 188-190°C. IR (KBr, ν cm^{-1}): 3440, 3316 (N-H), 2965, 2858 (C-H), 1651 (C=O), 1561

(C=N). ^{1}H-NMR (DMSO-d_6, δ ppm): 8.51 (d, 1H, Ar-H), 8.44 (d, 1H, Ar-H), 8.24 (d, 1H, Ar-H), 7.77-7.76 (m, 1H, Ar-H), 7.72 (s, 1H, Ar-H), 7.45 (dd, 1H, Ar-H), 6.51 (s, 2H, NH_2), 3.77-3.75 (m, 4H, OCH_2), 3.24-3.21 (m, 4H, CH_2), 2.45 (s, 3H, CH_3). ^{13}C-NMR (DMSO-d_6, δ ppm): 164.55, 153.30, 145.85, 140.55, 138.96, 138.32, 133.70, 131.09, 130.52, 122.40, 120.65, 120.28, 115.22, 65.86, 47.61, 20.93. ESI-MS (m/z): 338.20 $[M+1]^+$.

(3-amino-5-methyl-1H-indazol-1-yl) (5-(pyrrolidin-1-yl)pyridin-3-yl)methanone (7j)

White crystalline solid; Yield: 65%; m.p.: 218-220°C. IR (KBr, ν cm^{-1}): 3435, 3312 (N-H), 2969, 2845 (C-H), 1659 (C=O), 1554 (C=N). ^{1}H-NMR (DMSO-d_6, δ ppm): 8.31 (s, 1H, Ar-H), 8.24-8.22 (d, 1H, Ar-H), 8.05-8.04 (d, 1H, Ar-H), 7.71-7.71 (m, 1H, Ar-H), 7.45-7.43 (m, 1H, Ar-H), 7.35-7.33 (m, 1H, Ar-H), 6.48 (s, 2H, NH_2), 3.39-3.28 (m, 4H, NCH_2), 2.45 (s, 3H, CH_3), 2.01-1.94 (m, 4H, CH_2). ^{13}C-NMR (DMSO-d_6, δ ppm): 165.02, 153.20, 136.88, 135.44, 133.60, 131.04, 130.48, 120.61, 120.25, 118.59, 115.22, 47.09, 24.90, 20.94. ESI-MS (m/z): 322.30 $[M+1]^+$.

In vitro Cell Line Studies

The cytotoxic activity of the synthesized compounds (7i and 7j) was evaluated using the Sulforhodamine B (SRB) assay, a standard method for estimating cell density based on cellular protein content. MCF-7 breast cancer cells were cultured in a growth medium supplemented with 10% fetal bovine serum and 2 mM L-glutamine. Approximately 5 × 10^3 cells were seeded in each well of a 96-well plate and incubated at 37°C in a humidified atmosphere containing 5% CO_2 for 24 hr. Following incubation, the test compounds were added at different concentrations, and the cells were further incubated. After treatment, cells were fixed, stained with SRB dye, and the absorbance was measured to determine cell viability. The percentage growth was calculated by comparing the absorbance of treated cells (Ti) with control cells (C), and growth inhibition was expressed as:

$$\% \text{ Growth} = (Ti / C) \times 100$$

(Kode *et al*., 2020; Kholiya *et al*., 2020; Vichai and Kirtikara, 2006; Skehan *et al*., 1990).

Molecular Docking Studies

Molecular docking studies were performed using AutoDock Vina to evaluate the binding affinity of compounds 7i and 7j with the target protein. The results demonstrated favorable binding interactions, indicating their potential as anticancer agents.

Protein Preparation

The three-dimensional structure of the target protein, human CDK7 in complex with Cyclin H and MAT1 (PDB ID: 5JFX), was retrieved from the Protein Data Bank. The structure was prepared using PyMOL and AutoDock Tools by removing water molecules, ions, and co-crystallized ligands. Hydrogen atoms were added, Kollman charges were assigned, and the protein was

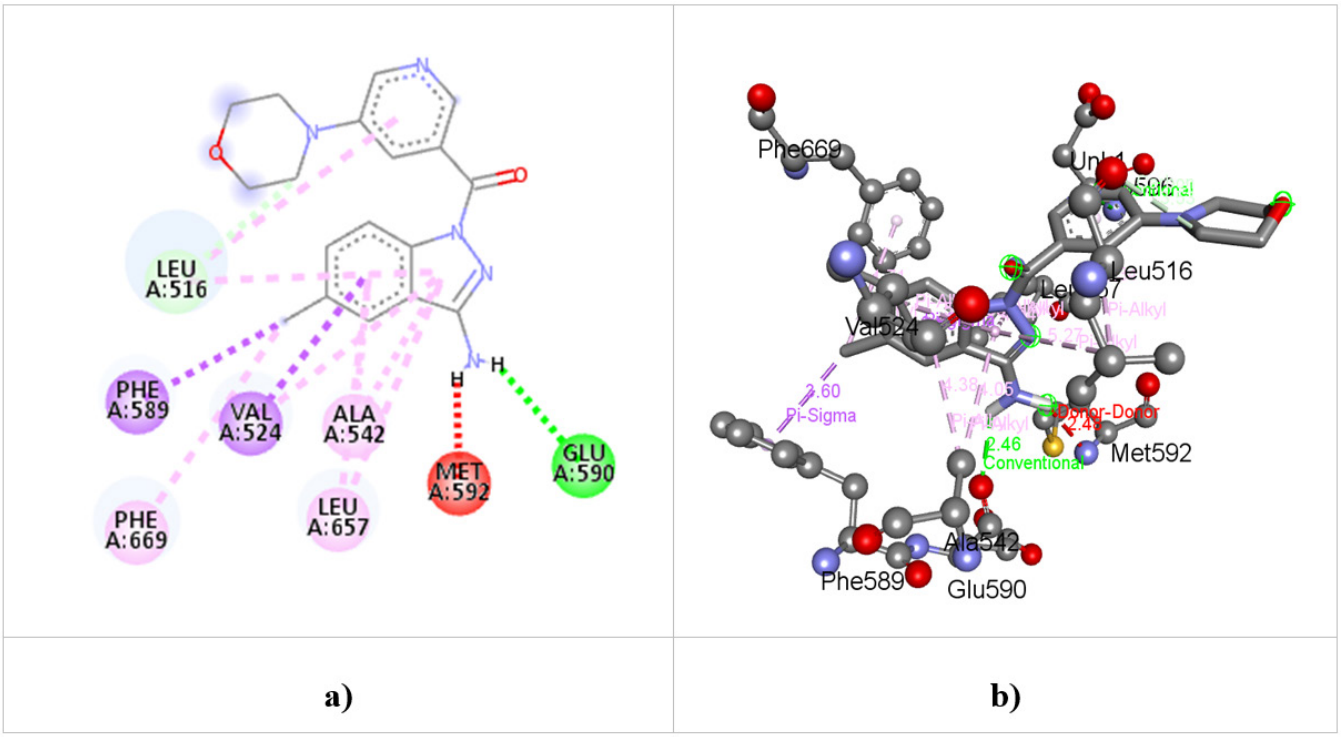

Figure 1: Docking Interaction of Compound 7i with Target Protein (5jfx). a) Binding interactions of 7i with a.a. residues of TrkA. b) Surface representation of 7i inside the binding pocket of TrkA receptor within the binding pocket of receptor (PDB: 5JFX). The TrkA receptor is expressed in the form of line diagram. The figures have been created using Discovery Studio Visualizer 2019. The amino acid residues are showed in black colour.

saved in PDBQT format for docking studies (Trott and Olson, 2010; Lipinski, 2016; Veber *et al*., 2002).

Ligand Preparation

The chemical structures of compounds 7i and 7j were drawn using ChemDraw Ultra 12.0 and energy minimized using Chem3D 12.0. The optimized structures were converted into PDB format for further processing.

Docking Procedure

The prepared ligands were converted into PDBQT format using AutoDock Tools 1.5.6. Docking simulations were carried out using AutoDock Vina, with the grid box set to 60 × 60 × 60 Å and an exhaustiveness value of 8. The grid was centered on the active site of the protein to allow optimal ligand interaction. Each ligand was docked individually, and the resulting conformations were analyzed based on binding energy (kcal/mol) and interaction patterns. The best docking poses were visualized using Discovery Studio Visualizer.

In silico ADME Studies

The pharmacokinetic properties of compounds 7i and 7j were predicted using the SwissADME online tool. Key parameters such as lipophilicity, solubility, gastrointestinal absorption, blood-brain barrier permeability, and CYP450 enzyme inhibition were evaluated. Drug-likeness was assessed based on Lipinski's Rule of Five and Veber's criteria, indicating their potential suitability for oral bioavailability (Daina *et al*., 2017).

RESULTS AND DISCUSSION

Rationale

Indazole and pyridine scaffolds are well-known for their pharmacological relevance, particularly in anticancer drug development. The integration of these heterocyclic systems offers the potential to enhance biological activity through improved binding interactions and modulation of key signaling pathways. In recent years, targeted therapies focusing on kinase inhibition have gained significant attention, particularly in breast cancer treatment. The present dataset was generated to explore the chemical and biological properties of two indazole-pyridine derivatives (7i and 7j). The rationale behind selecting these compounds lies in the incorporation of different cyclic amine substitutions (morpholine and pyrrolidine), which are expected to influence physicochemical properties such as lipophilicity, solubility, and biological activity. This data article provides comprehensive experimental and computational datasets, including synthesis protocols, spectral characterization, molecular docking results, and *in vitro* anticancer evaluation. These datasets are valuable for researchers working in medicinal chemistry and drug design, as they offer insights into structure-activity relationships and potential optimization strategies.

Chemistry

The target indazole-pyridine derivatives (7i and 7j) were successfully synthesized via a multi-step synthetic route and obtained in good yields. The structures were confirmed using FTIR, ^{1}H-NMR, ^{13}C-NMR, and ESI-MS analysis. Both compounds exhibited characteristic IR peaks corresponding to N-H stretching (~3300-3400 cm^{-1}) and a strong carbonyl (C=O) band around 1650 cm^{-1}. The ^{1}H-NMR spectra showed aromatic

Table 1: Physicochemical Properties of Synthesized Compounds.

Compound	Molecular Formula	Yield (%)	M.P (°C)	R_f Value
7i	$C_{18}H_{19}N_5O_2$	67	188-190	0.26
7j	$C_{18}H_{19}N_5O$	65	218-220	0.34

Table 2: Molecular properties of synthesized compounds.

Compd Code	Lipinski Rule of Five						Veber Rule		
	MW	HBA	HBD	MLogP	nviolations	DL	nRB	TPSA	DL
Rule	≤ 500	≤ 10	≤ 5	≤ 4.15	≤ 1	Yes	≤ 10	≤ 140	Yes
7i	337.38	4	1	1.97	0	Yes	3	86.27	Yes
7j	321.38	3	1	2.77	0	Yes	3	77.04	Yes

Note: MW - Molecular weight (g/mol), HBA - No. of H-bond acceptor, HBD - No. of H-bond donor, nRB - No. of rotatable bonds, TPSA - Topological Polar Surface Area (Å^2), DL - Drug-likeliness.

Table 3: Pharmacokinetic properties of synthesized compounds (7i-7j).

Comp. code	GI absorption	BBB permeation	Pgp substrate	CYP1A2	CYP2C19	CYP2C9	CYP2D6
7i	High	No	Yes	No	No	Yes	No
7j	High	Yes	Yes	Yes	No	Yes	No

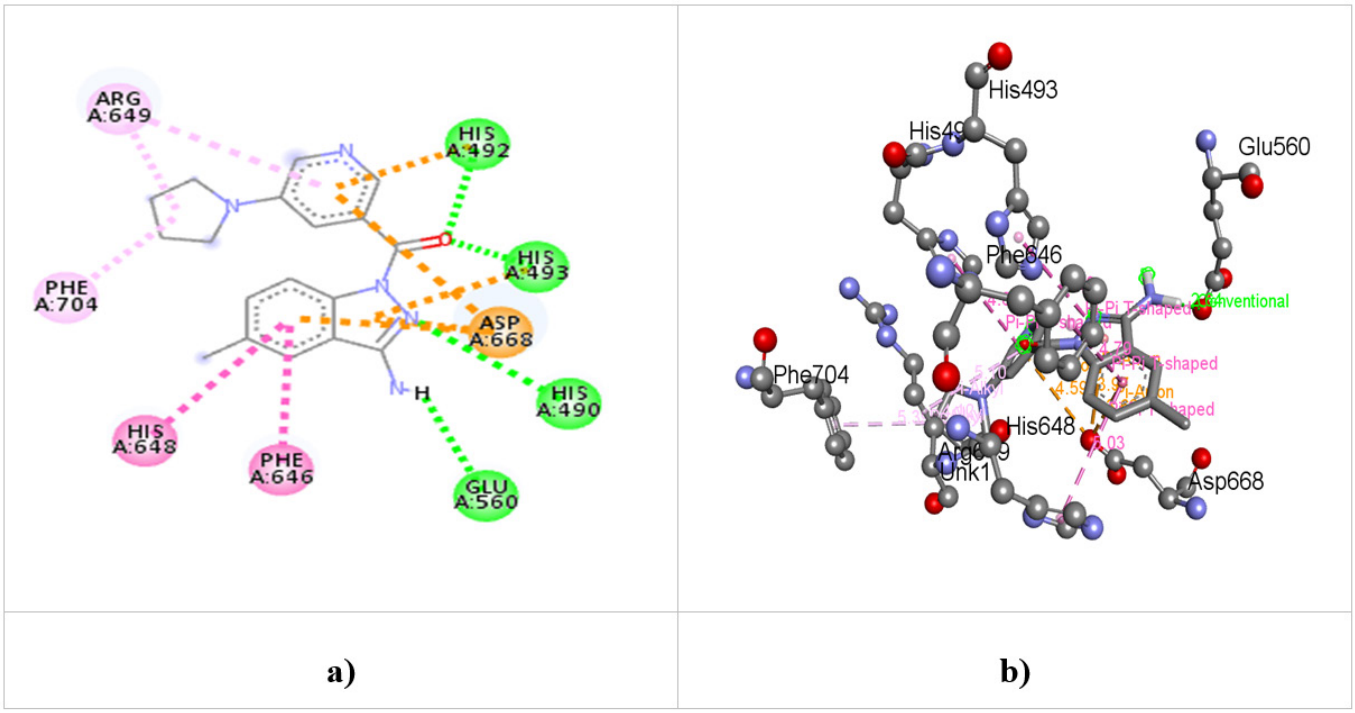

Figure 2: Docking Interaction of Compound 7j with Target Protein (5jfx). a) Binding interactions of 7j with a.a. residues of TrkA. b) Surface representation of 7j inside the binding pocket of TrkA receptor within the binding pocket of receptor (PDB: 5JFX). The TrkA receptor is expressed in the form of line diagram. The figures have been created using Discovery Studio Visualizer 2019. The amino acid residues are shown in black colour.

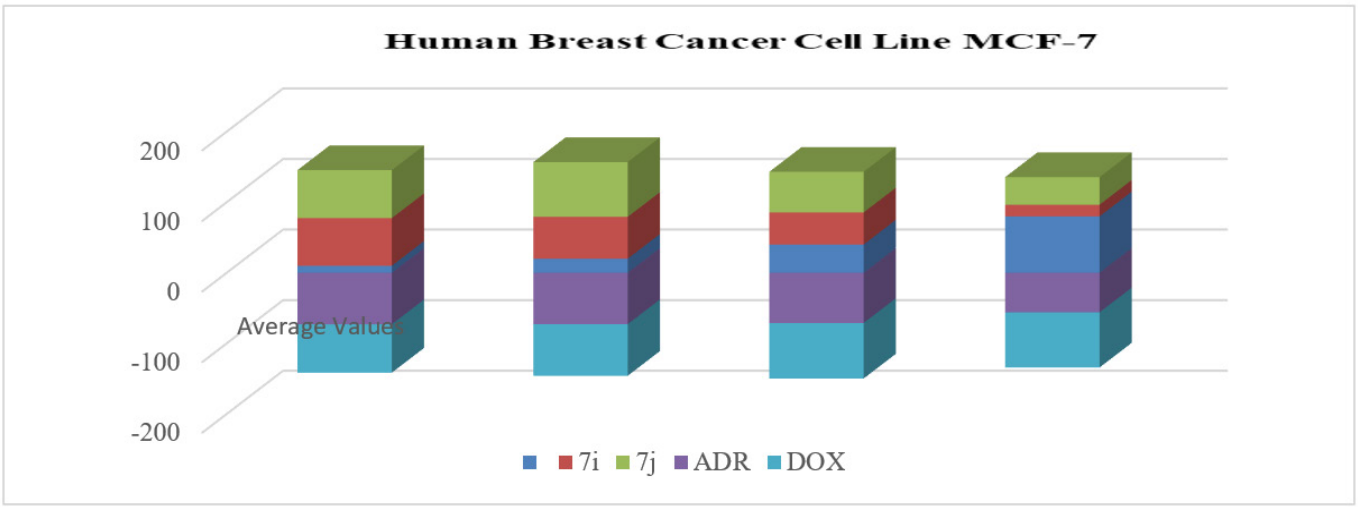

Figure 3: Growth inhibition curve of MCF-7 human breast cancer cells treated with synthesized compounds (7i-7j), Doxorubicin, and ADR. This figure illustrates the dose-dependent effects of various synthesized compounds (7i-7j) on the proliferation of MCF-7 breast cancer cells. The growth inhibition was measured at four different concentrations: 10, 20, 40, and 80 µg/mL, and expressed as % control growth.

protons in the range of δ 7.0-8.5 ppm, along with signals for NH_2 (~6.5 ppm) and methyl groups (~2.4 ppm). Compound 7i displayed additional signals corresponding to the morpholine ring, whereas compound 7j showed peaks characteristic of the pyrrolidine moiety. The ^{13}C-NMR and mass spectra further confirmed the proposed structures. The physicochemical properties of the synthesized compounds are presented in Table 1, while their molecular properties are summarized in Table 2. The predicted pharmacokinetic parameters are shown in Table 3.

Molecular Docking Studies

Docking studies were performed to evaluate the interaction of compounds 7i and 7j with the target protein. Both compounds showed good binding affinity and stable interactions within the active site. The detailed binding energies obtained from molecular docking studies are listed in Table 4. Compound 7i exhibited a binding energy of -8.5 kcal/mol, indicating strong interaction with the protein, possibly through hydrogen bonding and π-π stacking interactions. Compound 7j showed a binding energy of

-6.5 kcal/mol, suggesting moderate binding affinity. The docking interactions of compounds 7i and 7j with the target protein are illustrated in Figures 1 and 2, respectively.

In vitro Anticancer Activity

The anticancer activity of compounds 7i and 7j was evaluated against the MCF-7 breast cancer cell line using the SRB assay. Both compounds exhibited dose-dependent cytotoxicity. The *in vitro* cytotoxicity data for the MCF-7 cell line are presented in Table 5, and the growth inhibition curve is depicted in Figure 3.

Table 4: Molecular Docking Results.

Compound	Binding Energy (kcal/mol)
7i	-8.5
7j	-6.5

Compound 7i demonstrated moderate activity with a GI_{50} value of 33.6 µg/mL, whereas compound 7j showed comparatively higher activity with a GI_{50} value of <10 µg/mL. The GI_{50} values of the synthesized compounds are summarized in Table 6. The morphological changes in MCF-7 cells after treatment with compounds 7i and 7j are shown in Figure 4, indicating apoptosis and cytotoxic effects.

Structure-Activity Relationship (SAR)

The structure-activity relationship of the synthesized compounds is illustrated in Figure 5. The biological activity of the synthesized

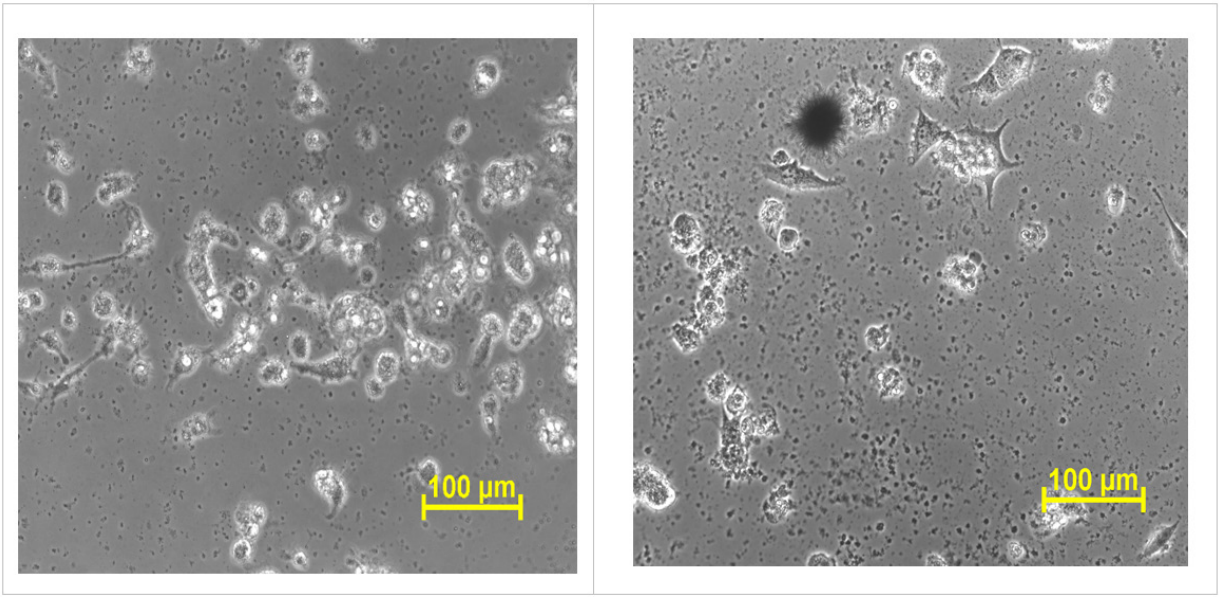

Figure 4: Describes the phase-contrast microscopy image of compound 7i and 7j for the MCF-7 breast cancer cell line. The rounded, detached, and vacuolated cells are strong indicators of apoptosis/cytotoxicity. The cell debris further supports ongoing cell death or stress response.

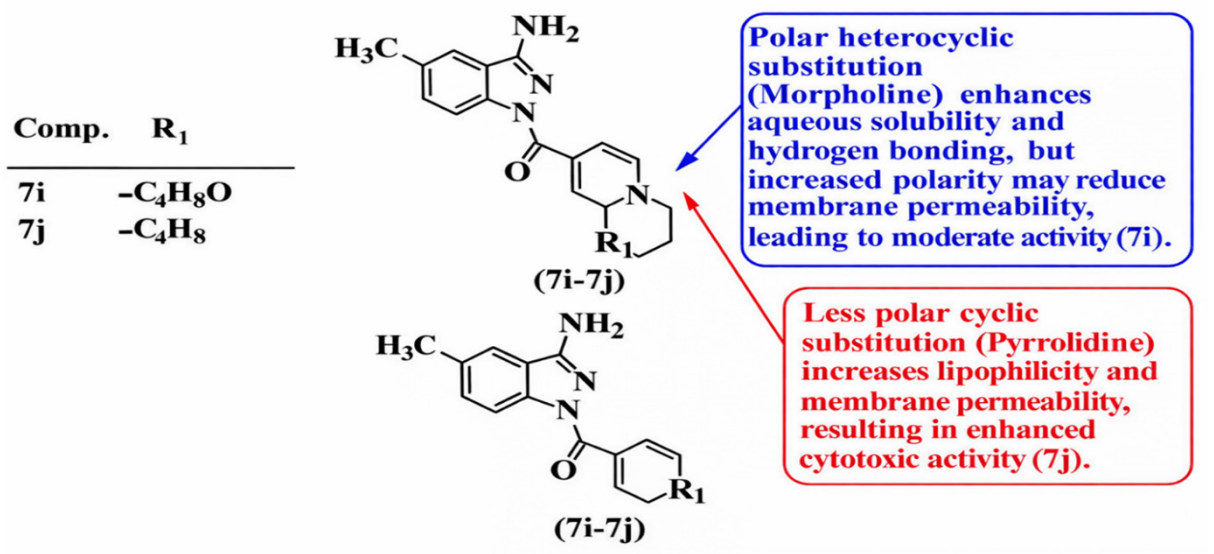

Figure 5: Structural Activity Relationship of synthesized compounds.

Table 5: Cell Line study: Human Breast Cancer Cell Line MCF-7.

	Human Breast Cancer Cell Line MCF-7															
	% Control Growth															
	Drug Concentrations (µg/mL)															
	Experiment 1				Experiment 2				Experiment 3				Average Values			
	10	20	40	80	10	20	40	80	10	20	40	80	10	20	40	80
7i	74.9	66.4	31.1	13.1	65.5	53.1	40.3	11.2	62.1	58.4	65.1	25.1	67.5	59.3	45.5	16.5
7j	57.3	63.9	45.6	30.0	68.8	79.1	63.4	45.1	78.0	89.6	63.9	42.2	68.0	77.6	57.6	39.1
ADR	-74.1	-72.7	-72.9	-52.5	-65.6	-68.9	-67.2	-55.6	-78.4	-75.3	-72.7	-59.2	-72.7	-72.6	-70.9	-55.8
DOX	-60.6	-69.4	-74.1	-72.6	-70.2	-73.5	-80.4	-80.5	-74.8	-76.5	-81.4	-81.5	-68.6	-73.1	-78.7	-78.2

Table 6: *In vitro* Anticancer Activity (MCF-7 Cell Line).

Compound	GI_{50} (µg/mL)
7i	33.6
7j	<10
Adriamycin (Std.)	<10
Doxorubicin (Std.)	<10

compounds was influenced by the nature of substituents on the pyridine ring. Compound 7i, containing a morpholine moiety, showed moderate activity, possibly due to increased polarity affecting membrane permeability. In contrast, compound 7j, bearing a pyrrolidine group, and exhibited enhanced cytotoxic activity. This may be attributed to improved hydrophobic interactions and better binding within the active site of the target protein. These findings suggest that less polar cyclic amines may enhance anticancer activity.

CONCLUSION

In this study, two indazole-pyridine derivatives (7i and 7j) were designed, synthesized, and evaluated for anticancer activity against the MCF-7 breast cancer cell line. Both compounds exhibited moderate cytotoxic effects, with compound 7j showing comparatively better activity. Molecular docking studies indicated favorable binding interactions with the target protein, supporting their potential as anticancer agents. However, further structural optimization is required to enhance potency and selectivity. These findings suggest that indazole-pyridine hybrids containing heterocyclic amines may serve as promising scaffolds for future anticancer drug development.

ACKNOWLEDGEMENT

The first author is thankful to Parul University, Vadodara, and Gujarat for providing intramural grant and providing infrastructure facility for the research work. Authors are thankful to Tata Institute of Fundamental Research (TIFR), Mumbai for conduction of *in vitro* cell-lines studies.

ABBREVIATIONS

ADME: Absorption, Distribution, Metabolism and Excretion; **ADR:** Adriamycin; **BBB:** Blood-Brain Barrier; **CDK7:** Cyclin-Dependent Kinase 7; **CYP:** Cytochrome P450; **DMF:** Dimethylformamide; **DMSO-d_6:** Deuterated Dimethyl Sulfoxide; **DOX:** Doxorubicin; **DPPE:** 1,2-Bis(diphenylphosphino)ethane; **EDC·HCl:** 1-Ethyl-3-(3-dimethylaminopropyl)carbodiimide Hydrochloride; **ESI-MS:** Electrospray Ionization Mass Spectrometry; **GI_{50}:** 50% Growth Inhibition Concentration; **HBA:** Hydrogen Bond Acceptors; HBD: Hydrogen Bond Donors; **HOBt:** Hydroxybenzotriazole; **MCF-7:** Michigan Cancer Foundation-7 Breast Cancer Cell Line; **NGF:** Nerve Growth Factor; **NTRK:** Neurotrophic Tyrosine Receptor Kinase; **PDB:** Protein Data Bank; **Pgp:** P-glycoprotein; **SAR:** Structure-Activity Relationship; **SRB:** Sulforhodamine B; **TIFR:** Tata Institute of Fundamental Research; **TPSA:** Topological Polar Surface Area; **TrkA:** Tropomyosin Receptor Kinase A.

CONFLICT OF INTEREST

The authors declare that there is no conflict of interest.

REFERENCES

Abbas, Z., and Rehman, S. (2018). An overview of cancer treatment modalities. *Neoplasm, 1*, 139-157.

André, F., Ciruelos, E., Rubovszky, G., Campone, M., Loibl, S., Rugo, H. S., and Juric, D. (2019). Alpelisib in breast cancer. *New England Journal of Medicine, 380*, 1929-1940.

Arruebo, M., Vilaboa, N., Sáez-Gutierrez, B., Lambea, J., Tres, A., Valladares, M., and González-Fernández, Á. (2011). Assessment of cancer treatment therapies. *Cancers, 3*(3), 3279-3330.

Berlin, J., Hong, D. S., Deeken, J. F., Boni, V., Oh, D. Y., Patel, J. D., and Drilon, A. (2020). Larotrectinib in GI cancer. *Cancer Research, 80*, CT052.

Charmsaz, S., Collins, D. M., Perry, A. S., and Prencipe, M. (2019). Novel strategies for cancer treatment. *Cancers, 11*(8), 1125.

Com, E., Lagadec, C., Page, A., El Yazidi-Belkoura, I., Slomianny, C., Spencer, A., and Hondermarck, H. (2007). TrkA signaling in breast cancer. *Molecular and Cellular Proteomics, 6*(11), 1842-1854.

Cui, J. J., Tran-Dubé, M., Shen, H., Nambu, M., Kung, P. P., Pairish, M., and Edwards, M. P. (2011). Structure-based drug design of crizotinib. *Journal of Medicinal Chemistry, 54*, 6342-6363.

Daina, A., Michielin, O., and Zoete, V. (2017). SwissADME tool. Scientific Reports, 7, 42717.

Davidson, B., Reich, R., Lazarovici, P., Florenes, V. A., Nielsen, S., and Nesland, J. M. (2004). NGF receptor expression in breast carcinoma. *Breast Cancer Research and Treatment, 83*, 119-128.

Descamps, S., Pawlowski, V., Révillion, F., Hornez, L., Hebbar, M., Boilly, B., and Peyrat, J. P. (2001). NGF receptor expression in breast cancer. *Cancer Research, 61*(11), 4337-4340.

Descamps, S., Toillon, R. A., Adriaenssens, E., Pawlowski, V., Cool, S. M., Nurcombe, V., and Hondermarck, H. (2001). NGF stimulates breast cancer cell proliferation. *Journal of Biological Chemistry, 276*(21), 17864-17870.

DiGiulio, S. (2013). FDA approves stivarga. *Oncology Times, 35*(6), 12.

Drilon, A., Siena, S., Dziadziuszko, R., Barlesi, F., Krebs, M. G., Shaw, A. T., and Doebele, R. C. (2020). Entrectinib clinical trials. *The Lancet Oncology, 21*, 261-270.

Federman, N., and McDermott, R. (2019). Larotrectinib review. *Expert Review of Clinical Pharmacology, 12*, 931-939.

Giaquinto, A. N., Sung, H., Newman, L. A., Freedman, R. A., Smith, R. A., Star, J., Jemal, A., and Siegel, R. L. (2024). Breast cancer statistics. *CA: A Cancer Journal for Clinicians, 74*, 465-519.

Helal, M. H., El-Awdan, S. A., Salem, M. A., Abd-Elaziz, T. A., Mohamed, Y. A., El-Sherif, A. A., and Mohamed, G. A. M. (2015). Pyridine derivatives as anticancer agents. *Spectrochimica Acta Part A, 135*, 764-773.

Kholiya, F., Chatterjee, S., Bhojani, G., Sen, S., Barkume, M., Kasinathan, N. K., and Meena, R. (2020). Seaweed nanocomposites. *Carbohydrate Polymers, 240*, 116282.

Knight, S. R., Shaw, C. A., Pius, R., Drake, T. M., Norman, L., Ademuyiwa, A. O., Adisa, A. O., *et al*. (2021). Global variation in postoperative mortality after cancer surgery. *The Lancet, 397*(10272), 387-397.

Kode, J., Kovvuri, J., Nagaraju, B., Jadhav, S., Barkume, M., Sen, S., and Kamal, A. (2020). Indole-linked chalcones. *Bioorganic Chemistry, 105*, 104447.

Kulothungan, V., Ramamoorthy, T., Sathishkumar, K., Mohan, R., Tomy, N., Miller, G. J., and Mathur, P. (2024). Burden of female breast cancer in India: Estimates of YLDs, YLLs, and DALYs. *Breast Cancer Research and Treatment, 205*, 323-332.

Lipinski, C. A. (2016). Rule of five revisited. *Advanced Drug Delivery Reviews, 101*, 34-41.

Liu, D., Offin, M., Harnicar, S., Li, B. T., and Drilon, A. (2018). Entrectinib overview. *Therapeutics and Clinical Risk Management, 14*, 1247-1252.

Lu, J., Blakely, C. M., Barve, M., Chung, C. H., Waqar, S. N., Hu, X., and Le Tourneau, C. (2022). Entrectinib in breast cancer. *Annals of Oncology, 33*, S204-S205.

Martin-Zanca, D., Hughes, S. H., and Barbacid, M. (1986). Human oncogene formation. *Nature, 319*, 743-748.

Noh, S. J., Bae, J. S., Jamiyandorj, U., Park, H. S., Kwon, K. S., Jung, S. H., and Jang, K. Y. (2013). NGF and HO-1 expression in breast carcinoma. *BMC Cancer, 13*, 516.

Roy, A., and Li, S. D. (2016). Modifying the tumor microenvironment using nanoparticle therapeutics. *Wiley Interdisciplinary Reviews: Nanomedicine and Nanobiotechnology, 8*(6), 891-908.

Siegel, R. L., Giaquinto, A. N., and Jemal, A. (2024). Cancer statistics, 2024. *CA: A Cancer Journal for Clinicians, 74*, 12-49.

Skehan, P., Storeng, R., Scudiero, D., Monks, A., McMahon, J., Vistica, D., and Boyd, M. R. (1990). Cytotoxicity assay. *Journal of the National Cancer Institute, 82*, 1107-1112.

Skerratt, S. E., Andrews, M., Bagal, S. K., Bilsland, J., Brown, D., Bungay, P. J., and Waldron, G. (2016). Pan-Trk inhibitor discovery. *Journal of Medicinal Chemistry, 59*, 10084-10099.

Trott, O., and Olson, A. J. (2010). AutoDock Vina. *Journal of Computational Chemistry, 31*, 455-461.

Veber, D. F., Johnson, S. R., Cheng, H. Y., Smith, B. R., Ward, K. W., and Kopple, K. D. (2002). Oral bioavailability properties. *Journal of Medicinal Chemistry, 45*, 2615-2623.

Vichai, V., and Kirtikara, K. (2006). SRB assay method. *Nature Protocols, 1*, 1112-1116.

Youssef, G., Gillett, C., Agbaje, O., Crompton, T., and Montano, X. (2014). Phosphorylation of NTRK1. *Modern Pathology, 27*, 361-374.

Cite this article: Parmar K, Panchal I. Experimental and Computational Data on Indazole-Pyridine Derivatives: Synthesis, Characterization, and Anticancer Evaluation. Asian J Biol Life Sci. 2026;15(2):559-66.